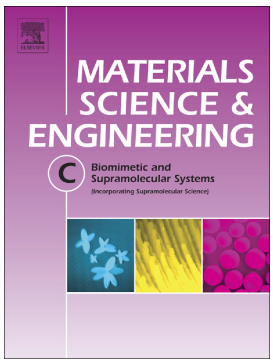

Macroporous click-elastin-like hydrogels for tissue engineering applications

Alicia Fernández-Colino, Frederic Wolf, Hans Keijdener, Stephan Rutten, Thomas Schmitz-Rode, Stefan Jockenhoevel, J. Carlos Rodríguez-Cabello, Petra Mela

PII: S0928-4931(17)33528-2
DOI: doi:10.1016/j.msec.2018.03.013
Reference: MSC 8434

To appear in: *Materials Science & Engineering C*

Received date: 1 September 2017
Revised date: 15 February 2018
Accepted date: 15 March 2018

Please cite this article as: Alicia Fernández-Colino, Frederic Wolf, Hans Keijdener, Stephan Rutten, Thomas Schmitz-Rode, Stefan Jockenhoevel, J. Carlos Rodríguez-Cabello, Petra Mela , Macroporous click-elastin-like hydrogels for tissue engineering applications. The address for the corresponding author was captured as affiliation for all authors. Please check if appropriate. Msc(2017), doi:10.1016/j.msec.2018.03.013

Macroporous Click-Elastin-Like Hydrogels for Tissue Engineering Applications.

*Alicia Fernández-Colino,[1] * Frederic Wolf,[1] Hans Keijdener,[1] Stephan Rutten,[2] Thomas Schmitz-Rode,[1] Stefan Jockenhoevel,[1] J. Carlos Rodríguez-Cabello,[3] Petra Mela.[1]**

[1]Department of Biohybrid & Medical Textiles (BioTex) at AME-Institute of Applied Medical Engineering, Helmholtz Institute & ITA-Institut für Textiltechnik, RWTH Aachen University, Pauwelsstr. 20, 52074. Aachen, Germany.

[2]Electron Microscopy Facility, Uniklinik RWTH Aachen, Pauwelsstrasse, 30, D-52074 Aachen, Germany

[3]Bioforge Lab, University of Valladolid, CIBER-BBN, Paseo de Belen 11, 47011 Valladolid, Spain.

* Corresponding Authors e-mail: fernandez@ame.rwth-aachen.de
mela@ame.rwth-aachen.de

ABSTRACT

Elastin is a key extracellular matrix (ECM) protein that imparts functional elasticity to tissues and therefore an attractive candidate for bioengineering materials. Genetically engineered elastin-like recombinamers (ELRs) maintain inherent properties of the natural elastin (e.g. elastic behavior, bioactivity, low thrombogenicity, inverse temperature transition) while featuring precisely controlled composition, the possibility for biofunctionalization and non-animal origin. Recently the chemical modification of ELRs to enable their crosslinking via a catalyst-free click chemistry reaction, has further widened their applicability for tissue engineering. Despite these outstanding properties, the generation of macroporous click-ELR

scaffolds with controlled, interconnected porosity has remained elusive so far. This significantly limits the potential of these materials as the porosity has a crucial role on cell infiltration, proliferation and ECM formation. In this study we propose a strategy to overcome this issue by adapting the salt leaching/gas foaming technique to click-ELRs. As result, macroporous hydrogels with tuned pore size and mechanical properties in the range of many native tissues were reproducibly obtained as demonstrated by rheological measurements and quantitative analysis of fluorescence, scanning electron and two-photon microscopy images. Additionally, the appropriate size and interconnectivity of the pores enabled smooth muscle cells to migrate into the click-ELR scaffolds and deposit extracellular matrix. The macroporous structure together with the elastic performance and bioactive character of ELRs, the specificity and non-toxic character of the catalyst-free click-chemistry reaction, make these scaffolds promising candidates for applications in tissue regeneration. This work expands the potential use of ELRs and click chemistry systems in general in different biomedical fields.

Keywords: Elastin; Elastin-like recombinamers; Macroporous scaffolds; Click-chemistry; Salt-leaching/gas foaming; Cell ingrowth

1. INTRODUCTION

One of the ongoing challenges in biomaterials science is the creation of scaffolds able to mimic the extracellular matrix (ECM) in the broadest sense, that is, recapitulating the bioactivity, the mechanical properties and the cytocompatibility,[1] besides meeting the requirements of porosity depending on the intended application.[2] Elastin is a key component of mammalian tissues which require elasticity to function in a physiological way and therefore, it is particular abundant in lungs, skin, blood vessels and elastic ligaments.

Furthermore, it displays inherent bioactivity and self-assembly properties.[3] These properties have positioned elastin as an attractive material in biomaterials science. However, the insoluble character of the natural elastin and its animal origin have limited its broad use for engineering scaffolds. The efforts to bring this material to the biomedical field have been materialized in the development of the elastin-like recombinamers (ELRs). ELRs are artificial polypeptides whose basic sequence is inspired by those found in the natural elastin. The amino-acid sequence of ELRs commonly comprises repeats of the (VPGXG) pentapeptide, where X can be any amino acid except proline. They are produced by genetic engineering techniques, [4] which ensures an absolute control over the amino acid composition and the achievement of a completely monodisperse material.[5] Furthermore, functional groups can be inserted in the repeating sequence obtaining in this way desired bioactive properties. ELRs have been shown to maintain important aspects of the natural elastin, such as the elastic behavior, the cytocompatibility,[6, 7] the low thrombogenicity [8-10] and the inverse transition behavior [11]. The later refers to a phase transition from soluble to insoluble that the ELR experiences in response to an environmental stimulus (e.g. pH, salt, or temperature). The transition temperature "Tt" is the specific temperature below which the polymer chain remains hydrated, and above which the ELR chain folds hydrophobically and forms a separate phase. ELRs are positioned midway between natural products and synthetic polymers, as they are engineered in a controlled and highly reproducible way while still mimicking the elastic and bioactive behavior of the natural elastin. All these properties explain the increasing interest for these materials in biomedical applications.[5, 12-14]

We have recently shown that ELRs could be chemically modified at their lysine groups to bear azide and cyclooctyne groups to enable the formation of hydrogels by a catalyst-free click chemistry reaction [15] . Click chemistry [16-19] (and concretely Huisgen 1,3-dipolar cycloadition of azides and alkynes) has proven itself to be superior to other crosslinking

approaches in many aspects: i) it displays high chemoselectivity, so that the reactant pairs are mutually reactive but do not cross-react with biological functionalities or interfere with reactions in cells [20], ii) the reaction works well under mild non-toxic conditions; iii) it displays short reaction time; iv) the chemical reactive groups are incorporated into the molecules intended to be crosslinked, and therefore there is no risk of the release of excess crosslinking reagents. The use of alkyne groups, such as cyclooctyne derivatives, has allowed these reactions to be carried out without the need of any catalyst, guaranteeing the cytocompatibility of the reaction.[21]

Despite the remarkable properties of these materials, their full potential remains still to be exploited as the creation of a controlled and interconnected porosity has not been achieved yet. This limits significantly the applicability of click-ELR-based scaffolds in tissue engineering where an interconnected porous architecture is required to assist in guiding and promoting new tissue formation, while facilitating the transport of nutrients and metabolites.[1] The capability of the scaffold to be infiltrated by cells and to support cell proliferation and ECM formation is essential whether the cells are seeded *in vitro* in classical bioreactor-based strategies[22, 23] or attracted to the scaffold *in vivo* once implanted, as envisioned by *in situ* tissue engineering approaches.[24-29] Matching porous properties is therefore a cornerstone in the development of scaffolds for tissue engineering

Among the several methods that have been reported to create porosity,[1] salt-leaching coupled with gas foaming (SL/GF) technique is considered as one of the best approaches since it offers the possibility not only to tune the pore-size but, importantly, to obtain an interconnected porous network.[30] This technique is based on the dispersion of a porogen (e.g. $NaHCO_3$ particles) with desired particle size into a polymer solution. Once the hydrogel has been crosslinked, the porogen particles are leached by immersing the material in mild acidic solution, resulting in the formation of CO_2 bubbles which ensures the

interconnectivity of the pores.[31] Despite the well-known advantages of this approach with respect to other strategies, the application of SL/GF technique to click chemistry hydrogels has proved elusive. This is due to the fact that SL/GF technique is performed in harmful organic solvents (DMF; DMSO) [30] while click-chemistry reactions are typically carried out in aqueous-based media in which the salt porogens have high solubility. Furthermore, high salt concentrations cause the transition of the ELR chain to an aggregated state. [11, 32, 33] This prevents the homogeneous mixture of the ELRs, ultimately leading to an irregular and non-reproducible crosslinked hydrogel. The aim of this study was to overcome the complications that both click chemistry and ELRs entail with respect to the SL/GF method to obtain scaffolds with controllable porosity. This implies choosing a dispersing medium that fulfills three requirements: i) it should enable the click chemistry reaction; ii) the solubility of the porogen (pore-forming agent) in it should be marginal; iii) it should hamper the transition behavior of the ELR.

The results described here demonstrate that we have overcome the challenge in obtaining click-ELR hydrogels with interconnected and tunable porosity by SL/GF. This opens a wide range of applications of these materials in tissue engineering and regenerative medicine.

2. MATERIALS AND METHODS

2.1. Differential Scanning Calorimetry (DSC)

DSC experiments were performed on a Mettler Toledo 822e with liquid-nitrogen cooler. Both temperature and enthalpy were calibrated with standard samples of indium and n-octane. The solutions for the DSC experiments were prepared by dissolving each ELR at 75 mg/ mL in aqueous buffered solution (PBS) or in the mixture of PBS/ ethanol 1:1 (v/v). 30 μL of the

solution was placed inside a standard 40-µL aluminum pan and sealed hermetically. The same volume of the employed solvent was placed in the reference pan. Both, sample and reference were heated at a constant velocity. The heating program for DSC experiments included an initial isothermal stage (5 min at 0 °C for stabilization of the temperature and the state of the recombinamers), followed by heating at 5 °C/min from 0 °C to the 60 °C. The enthalpy values of endothermic processes were taken as negative and exothermic as positive.

2.2. Scaffold fabrication

Two ELRs, namely VKVx24 and HRGD6, were employed. VKVx24 is a structural recombinamer with no bioactive sequence and HRGD6 is a recombinamer containing a RGD adhesion sequence (Table 1). The ELRs were chemically modified as previously reported[15] at their lysine amino acids to bear the reactive groups necessary for subsequent click chemistry reactions, namely cyclooctyne and azide. The modified versions of these ELRs are referred to in the present work as VKVx24-c and HRGD6-a.

Table 1: Amino acid sequence of each recombinamer and the corresponding reactive group used for the click chemistry reaction. Such reactive groups were incorporated by chemically modification of the lysines.

ELR	Amino acid sequence	Reactive group
VKVx24-c	MESLLPVGVPGVG[VPGKG$(VPGVG)_5]_{23}$VPGKGVPGVGVPGVGVPG VGVPGV	Cyclooctyne
HRGD6-a	MGSSHHHHHHSSGLVPRGSHMESLLP[$(VPGIG)_2$(VPGKG)$(VPGIG)_2$] $_2$AVTGRGDSPASS [$(VPGIG)_2$(VPGKG)$(VPGIG)_2]_2$	Azide

Each ELR component was dissolved at 75 mg/ mL in a mixture of PBS/ ethanol 1:1 (v/v). $NaHCO_3$ particles were added in a recombinamer/ salt weight ratio of 1:10 to each ELR

solution. Each preparation was loaded into a syringe, and injected into the mold by using a dual chamber syringe applicator (Figure 2). After 30 min at 37 ^{o}C, the mold was removed, and the click-ELR scaffold was released and placed in an acidic solution (citric acid 3M) for 30 min in an ultrasound bath[30]. The scaffolds were washed with aqueous buffer saline (PBS) to eliminate possible remains of ethanol, salts or acid. $NaHCO_3$ particles of three different sizes ranges (i.e. <40, <100 and 40-100 μm respectively) were used. Sterilization was performed by washing the scaffolds with ethanol 70% for 30 min and then keeping them in fresh ethanol 70% overnight. Finally, a series of baths in PBS (two baths of 30 min each, followed by one bath of 16 h) and DMEN (first bath 30 min, second bath 16 h) were carried out.

2.3. Brightfield and fluorescence microscopy

Samples were rinsed in PBS, fixed in Carnoy's fixative, embedded in paraffin and sectioned at 3 μm thickness. Sections were observed with a microscope equipped for epi-illumination (AxioObserver Z1; Carl Zeiss GmbH). Images were acquired using a digital camera (AxioCam MRm; Carl Zeiss GmbH). Pore size was measured by ImageJ software. For each fixed condition, three different regions were analyzed, by taking 50 measurements in each region.

2.4. Scanning Electron Microscopy (SEM)

Samples for SEM investigation were fixed in 3% glutaraldehyde in 0.1 M Sorenson's buffer (pH 7.4) at room temperature for 1 h. They were rinsed with sodium phosphate buffer (0.2 M, pH 7.39, Merk) and dehydrated consecutively in 30%, 50%, 70% and 90% acetone and then

three times in 100% acetone for 10 min. After critical point drying in CO_2, they were sputter-coated (Leica EM SC D500) with a 20 nm gold–palladium layer. Images were obtained with an ESEM XL 30 FEG microscope (FEI, Philips, Eindhoven, the Netherlands) with an accelerating voltage of 10 kV. Pore size was measured by ImageJ software. For each fixed condition, three different regions were analyzed, by taking 50 measurements in each region.

2.5. Two Photon Laser Scanning Microscopy (TPLSM)

Porosity of the resulting scaffolds and cell infiltration were further investigated using a two-photon laser scanning microscope (TPLSM). The set-up consisted of an Olympus FluoView 1000MPE with a 25x water objective (NA 1.05, Olympus, Tokyo, Japan), a mode-locked MaiTai DeepSee Titanium-Sapphire Laser (Spectra-Physics, Stahnsdorf, Germany), and the FluoView FV10 4.2 acquisition software. An excitation wavelength of 800 nm was used. The click-ELR hydrogels in their hydrated native state were visualized due to their auto-fluorescence. For the cell visualization, the seeded click-ELR hydrogels were fixed in methanol for 1h at -20 C, washed with PBS and incubated with propidium iodide (PI) at 20 µg/ mL in PBS for 5 min following by extensive washing in PBS to remove the excess of PI. Z-stacks produced with the TPLSM were rendered in Imaris (Bitplane, Zurich, Switzerland) image processing software. Pore size was measured by ImageJ software. For each fixed condition, three different regions were analyzed, by taking 50 measurements in each region.

2.6. Rheology

The mechanical properties of the hydrogels were determined using rheological tests in a strain-controlled rheometer (AR2000ex, TA Instruments).

Hydrogels hydrated in PBS were measured in the rheometer at 37 °C using a parallel plate geometry (12 mm diameter). Measurements of G' (elastic or storage modulus) and G" (viscous or loss modulus) were performed always within the linear viscoelastic region by varying the frequency (between 0.1 and 10 Hz) in a constant strain mode (0.5%).

2.7. Cell isolation and culture

SMCs were isolated from veins of human umbilical cords as previously described[34]. The umbilical cords were kindly provided by the Department of Gynecology at the University Hospital Aachen in accordance with the human subjects approval of the ethics committee (votum of the local ethics committee: #EK 2067). Briefly, the vein was washed with phosphate buffered saline (PBS; Gibco) before removing endothelial cells by using 1 mg/mL collagenase (Sigma). For isolation of the mixed population of SMCs/fibroblasts, the digested vein was minced into 1-mm rings and then bathed in the primary cell culture media Dulbecco's modified Eagle's medium (DMEM; Gibco) supplemented with 10% FBS (Gibco) and 1% antibiotic/antimycotic solution (Gibco). To obtain a sufficient number, the cells were serially passaged using 0.25% trypsin/0.02% EDTA solution (Gibco) and cultured in 5% CO_2 and 95% humidity at 37 ^{o}C. Cell passages 4-7 were used for all the experiments.

To study the interaction between the cells and the click-ELR hydrogels, disc-shaped porous ELR-scaffolds were placed in 96-well tissue culture plates and $3x10^4$ cells suspended in a volume of 100 µL were seeded on each hydrogel disc. The hydrogels were incubated for 6h with the saturated cell suspension to allow cell attachment. Then, the remaining cell suspension was removed, and fresh culture medium was added. Cell behavior was investigated by TPLSM and SEM after 3 and 11 days in culture.

2.8. Immunohistochemistry

Nonspecific sites on Carnoy's-fixed, paraffin-embedded sections from native human umbilical cord and click-ELR scaffolds were blocked and the cells were permeabilized with 5% normal goat serum (NGS, Dako) in 0.1% Triton-PBS. Sections were incubated for 1 h at 37 °C with a dilution 1:200 of the primary antibody rabbit anti-collagen I (R 1038, Acris). The sections were incubated for 1 h at 37 °C with a 1:400 dilution of a fluorescein-conjugated secondary antibody produced in rabbit (A11008, Molecular Probes). The native human umbilical cord served as a positive control. For negative controls, samples were incubated in diluent and the secondary antibody only. Tissue sections were counterstained with 4',6-diamidino- 2-phenylindole (DAPI) nucleic acid stain (Molecular Probes). Samples were observed with a microscope equipped for epi-illumination (AxioObserver Z1, Carl Zeiss GmbH). Images were acquired using a digital camera (AxioCam MRm, Carl Zeiss GmbH).

3. RESULTS AND DISCUSSION

3.1. Evaluation of the transition behavior of ELRs on different dispersing media

The transition behavior of the ELRs bearing the reactive groups for the click chemistry was investigated in two different dispersing media (PBS and a mixture of PBS/ethanol) by DSC. DSC has proven to be an adequate technique to evaluate the transition behavior, providing values for both the Tt and latent heat (ΔH). Figure 1a shows that the thermograms of the ELRs in PBS were characterized by the presence of an endothermic peak at 15.4 °C and 17.3 °C for VKVx24-c and HRGD6-a respectively. These peaks are associated with the inverse temperature transition (ITT) behavior characteristic of this kind of polymers and are in agreement with previously reported measurements.[15] However, such thermal performance

changed drastically when a mixture of PBS/ethanol was used as dispersing medium. Under such condition, no endothermic peak was observed, which points to the blockage of the ITT behavior of the ELRs. These results were further verified by the visual inspection of the corresponding solutions, in which both ELRs displayed an aggregated state in PBS and at RT, whereas they remained in a completely soluble state in PBS/ethanol (Figure 1b).

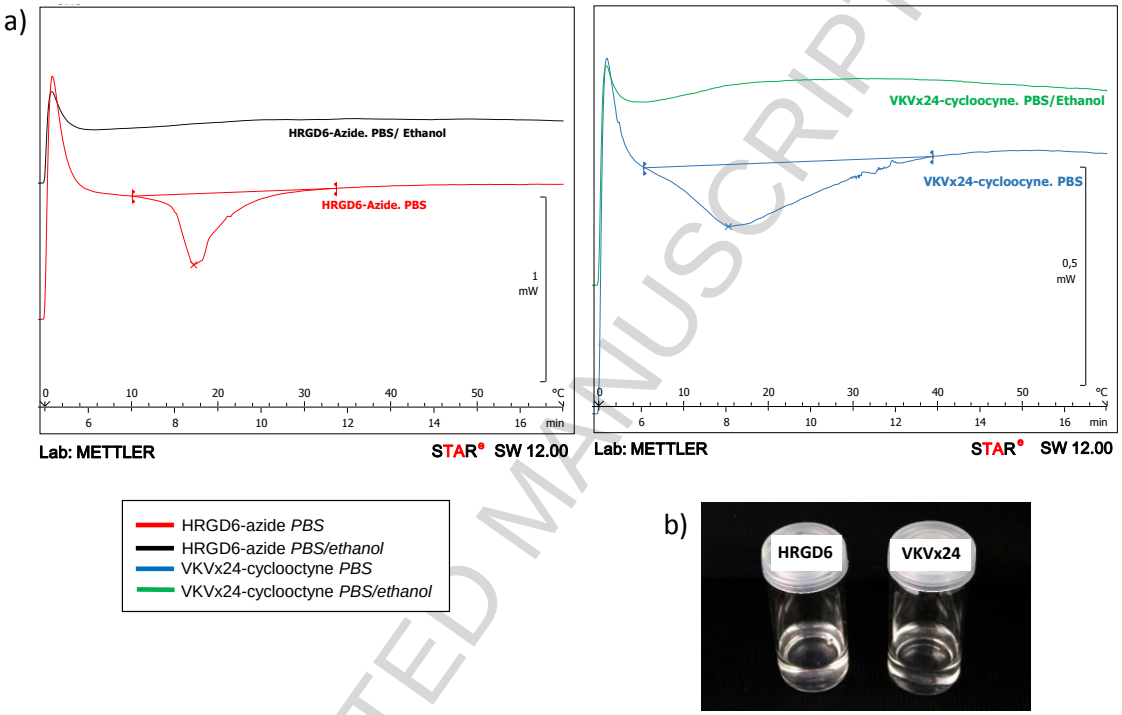

Figure 1. (a) DSC scans for VKV-cyclooctyne and RGD-azide in PBS and in a mixture or PBS/ethanol 1:1 (v/v). (b) Pictures showing the soluble state of the both recombinamers at room temperature when PBS/ ethanol is used as dispersing medium.

In light of the above, a complete dissolution of both recombinamers can be achieved at room temperature which facilitates their handling and mixing. Importantly, under these conditions, the use of salts as porogens is also permitted as the solubility of salts in mixtures of ethanol/ water has been reported to be negligible.[35] These findings pave the way for the application of the SL/GF approach to the click-ELR system.

3.2. Fabrication of macroporous click-ELR scaffolds

Disk-shaped scaffolds were fabricated by injection moulding technique following the approach depicted in Figure 2. The achievement of a hydrogel by mixing both components supported the feasibility of the click chemistry approach used in this system to be performed in the mixture of PBS/ethanol. Although click chemistry reactions had been reported to be compatible with aqueous-alcohol media,[36, 37] the use of these media for bioengineering purposes has not been exploited to any extend.

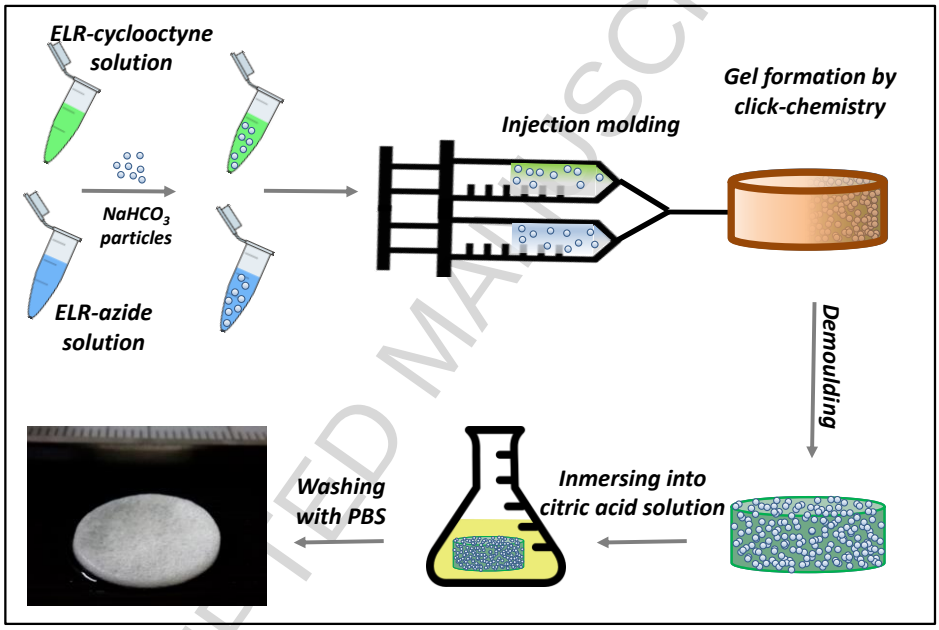

Figure 2. Sketch of the procedure followed to obtain the macroporous click-ELR hydrogels.

Microscopic inspection of the obtained hydrogels revealed that highly porous scaffolds were obtained for all the different size ranges of the porogen ($NaHCO_3$ particles) tested (Figure 3) which supports the robustness of the technique. All scaffolds appeared to have a homogeneous porous structure.

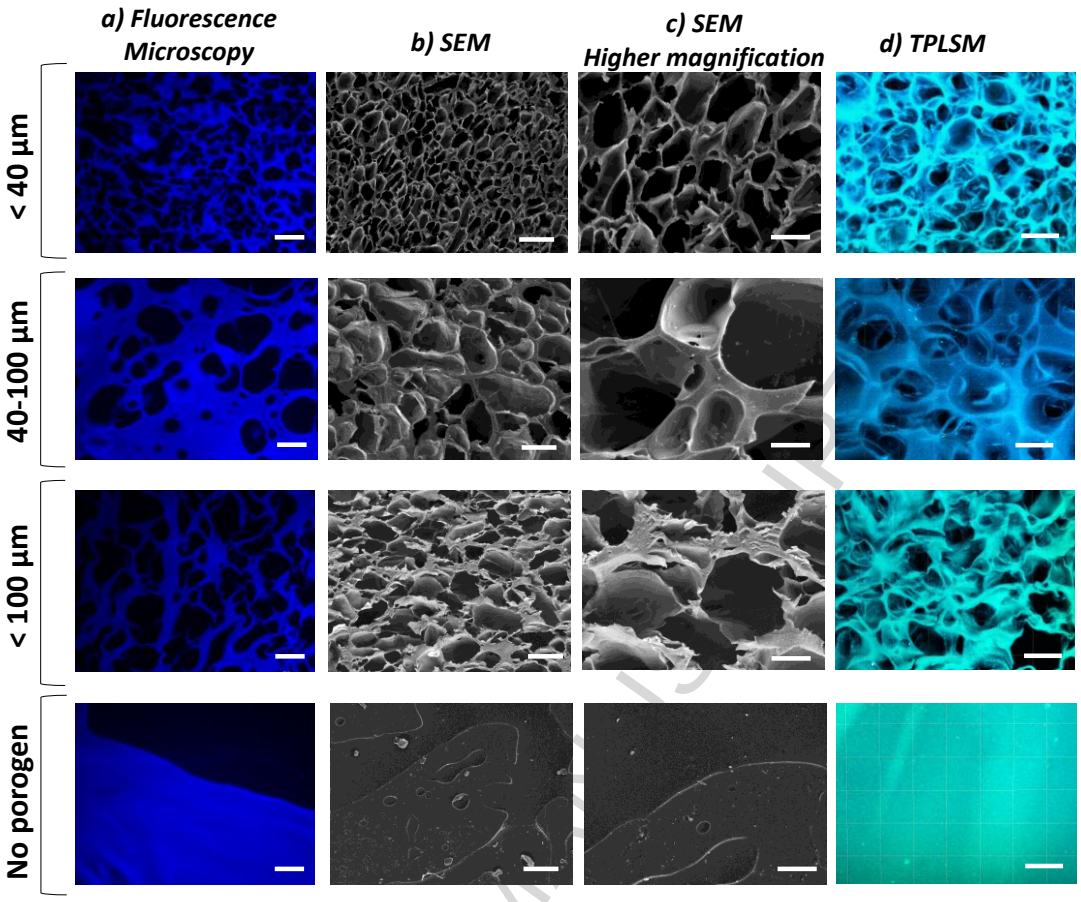

Figure 3. Porous characteristics of the click-ELR scaffolds prepared by SL/GF technique, according to the porogen´s size range specified on the left. (a) Fluorescence microscopy images of cuts of the paraffin embedded click-ELR scaffolds. (b) SEM images of click-ELR scaffolds. (c) Zoomed in views of the SEM images of the click-ELR scaffolds in hydrated state. (d) TPLSM images of click-ELR scaffolds. Scale bars: (a), (b) and (d) 50 µm; (c) 20 µm.

Quantitative analysis of the pore sizes was performed on images obtained by three different techniques (i.e. critical point drying followed by SEM, paraffin embedding followed by fluorescence microscopy and inspection of the hydrated state by TPLSM) (Figure 4a). A good correlation between the size range of the sieved particles and the scaffold's pore size was obtained in all cases. The slight differences in size detected for each experimental condition depending on the analytical technique used are likely due to both

vacuum/preparation defects on the gels during SEM operation and paraffin embedding, besides the different cross sections of the gel used for each measurement. But importantly, the same trend was observed for all the three techniques. As TPLSM allowed the visualization of the hydrogels in their hydrated state, the values provided by it were considered as the most accurate ones. The average pore sizes obtained by using TPLSM for the three ranges of $NaHCO_3$ particles were 24.3, 38.0 and 58.6 µm. These pore sizes are in the range of the recommended values for cell culture of fibroblastic cells,[24] which are the predominant cell type of connective tissues. The standard deviations of the mean pore size of three different regions were very low (as shown in Figure 4: 3,0; 0,7 and 7.0 µm for the particle range <40, <100 and 40-100 µm, respectively), which further supports the homogeneity of the porous structures created along the whole scaffold.

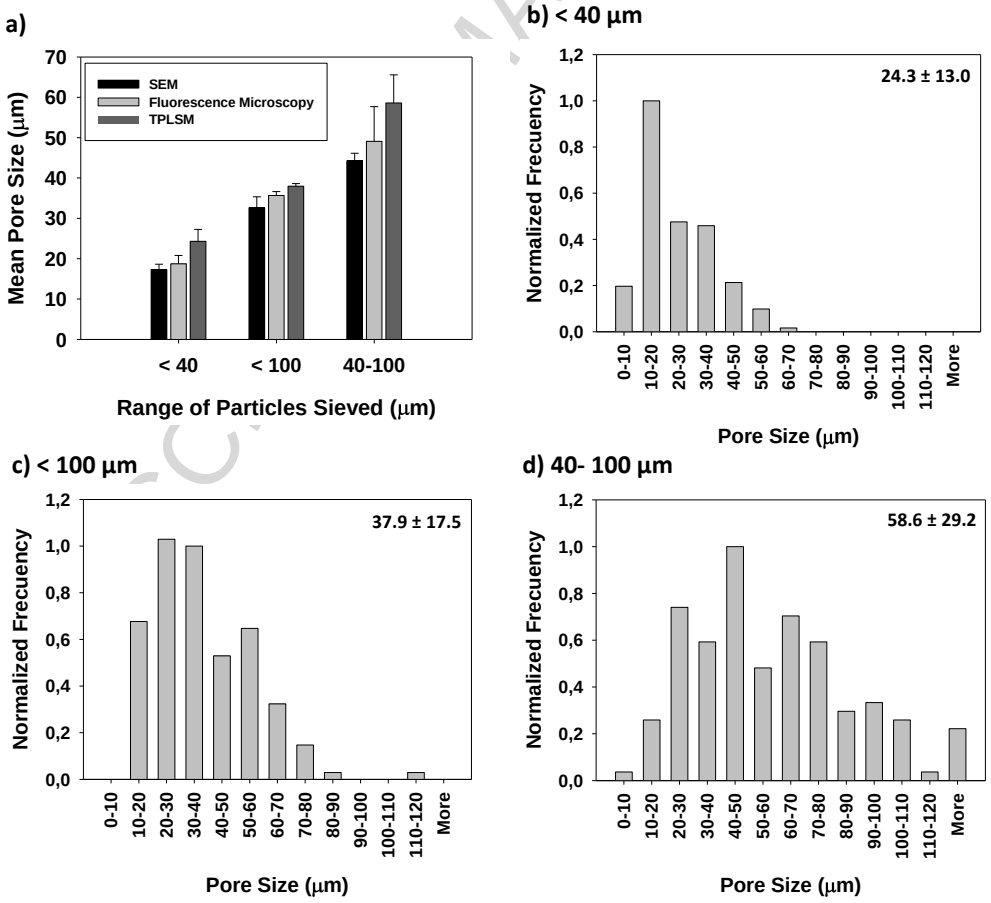

Figure 4. Quantitative analysis of the pore sizes. (a) Comparison of the pore size according to the range of $NaHCO_3$ particles sieved. Data was obtained by analyzing TPLSM, SEM and fluorescence microscopy images by ImageJ. Results are expressed as mean ± standard deviation of the average pore size of three different regions (n=3 regions, 50 measurements in each region). (b) Pore size distribution displayed by click-ELR hydrogels prepared by using a porogen size range < 40 μm. (c) Pore size distribution displayed by click-ELR hydrogels prepared by using a porogen size range < 100 μm. (d) Pore size distribution displayed by click-ELR hydrogels prepared by using a porogen size range 40- 100 μm. (b)-(c) Data was obtained by analyzing TPLSM images by ImageJ software. Mean ± standard deviation (n= 150 measurements) are indicated in the right upper corner of each plot.

The pore-size distribution obtained by analyzing TPLSM images for each experimental condition is provided in Figure 4b-c. For the three tested conditions, the scaffolds displayed a mix of large and small pores, with average pore sizes for each condition significantly different ($p<0.05$, n=150 measurements). Importantly, the coexistence of different pore sizes within the same scaffold may benefit its performance, as it has been suggested that such dispersion may be needed to promote a combination of tissue regenerative behaviors, such as infiltration and ECM secretion.[38] Concretely, it has been reported that pore sizes smaller than 12.5 μm can promote ECM production, while pores bigger than 20 μm are required for cell infiltration.[39] The pore size distribution has its basis on the experimental conditions used, in which a monodisperse population of salt particles was not sieved, but a polydisperse one.

3.3. Mechanical properties

Rheological tests were performed in order to evaluate the mechanical performance of the macroporous hydrogels. All the macroporous hydrogels displayed modulus around 2-4 kPa

(Figure 5), with no statistical differences for the different pore size ranges. Hydrogels in which no porosity was created displayed significantly higher values (7.5 kPa, Figure 5), which can be explained with the large amount of void volume in the porous scaffolds. Importantly, the tanδ values for all samples, regardless of the pore size, were in the range of 0.09 and therefore G´>> G´´, which means all the hydrogels displayed a viscoelastic character with a clear predominance of the elastic component (G´) over the loss component (G´´). As such, the elastic performance of the hydrogels was preserved after the SL/GF procedure.

Importantly, the mechanical performance of the hydrogels approximates those of many biological tissues [40] and are therefore appropriate as substrates to mimic the natural mechanical environment for cell studies and tissue engineering purposes.[2, 41, 42] This finding together with the macroporous structure and the RGD adhesion motif engineered in the recombinamer HRGD6-a points to a compatible scenario for cell ingrowth into the click-ELR hydrogel. The next set of experiments was designed to test such hypothesis.

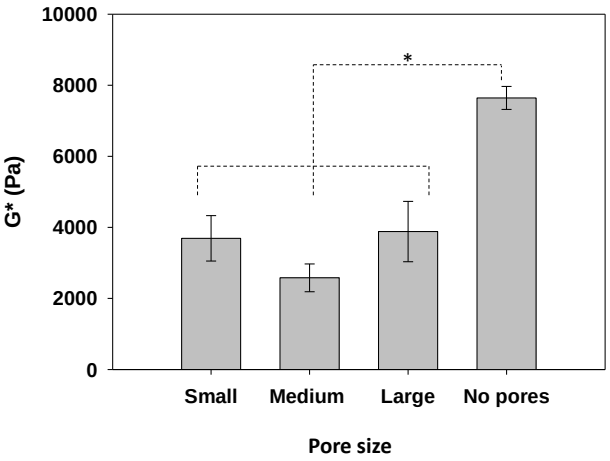

Figure 5. Mechanical properties as a function of pore size at 1 Hz and 37 °C. Data are reported as mean ± SD (n = 3). Statistical analysis was evaluated by analysis of variance using the Holm–Sidak method. *p < 0.05. Small, medium and large are referred to the

scaffolds obtained after sieving particles ranging from <40, <100 and 40-100 μm respectively.

3.4. Cell ingrowth and ECM production

Smooth muscle cells (SMCs) were seeded on scaffolds prepared by using salt particles with sizes < 100 μm and therefore exhibiting a mean pore size of 38 μm, which has been indicated as optimal for the interaction with SMCs[24]. As shown in Figure 6a) and b), SMCs presented a clear spread morphology, suggesting a tight interaction with the scaffold. Moreover, the comparison between two different culture-times (3 days and 11 days) clearly showed an increase in the number of cells colonizing the scaffolds. The cability of the ELR hydrogels to support cell proliferation is in agreement with previous studies in which human fibroblasts from the foreskin and human umbilical vein endothelial cells seeded on ELRs showed a population doubling time (PDT) of 34-48 h and 40-75 h respectively, as estimated from [8, 43]. In the present study, we have estimated PDT of 72-96 h, which is in accordance with the proliferation rate reported in the literature for human vein SMCs [44]

Additionally, the cells were not confined to the surface of the click-ELR scaffold, but they were able to infiltrate through the pores (Figure 6c), which provides evidence of the suitability of the pore size to support cell colonization. Moreover, the deposition of ECM was also patent (Figure 6d). This performance fits excellently with the two current philosophies encountered nowadays in tissue engineering (i.e. classical approach and *in situ* tissue engineering). In both, the capability of the scaffold to be infiltrated and to support proliferation is essential.[45]

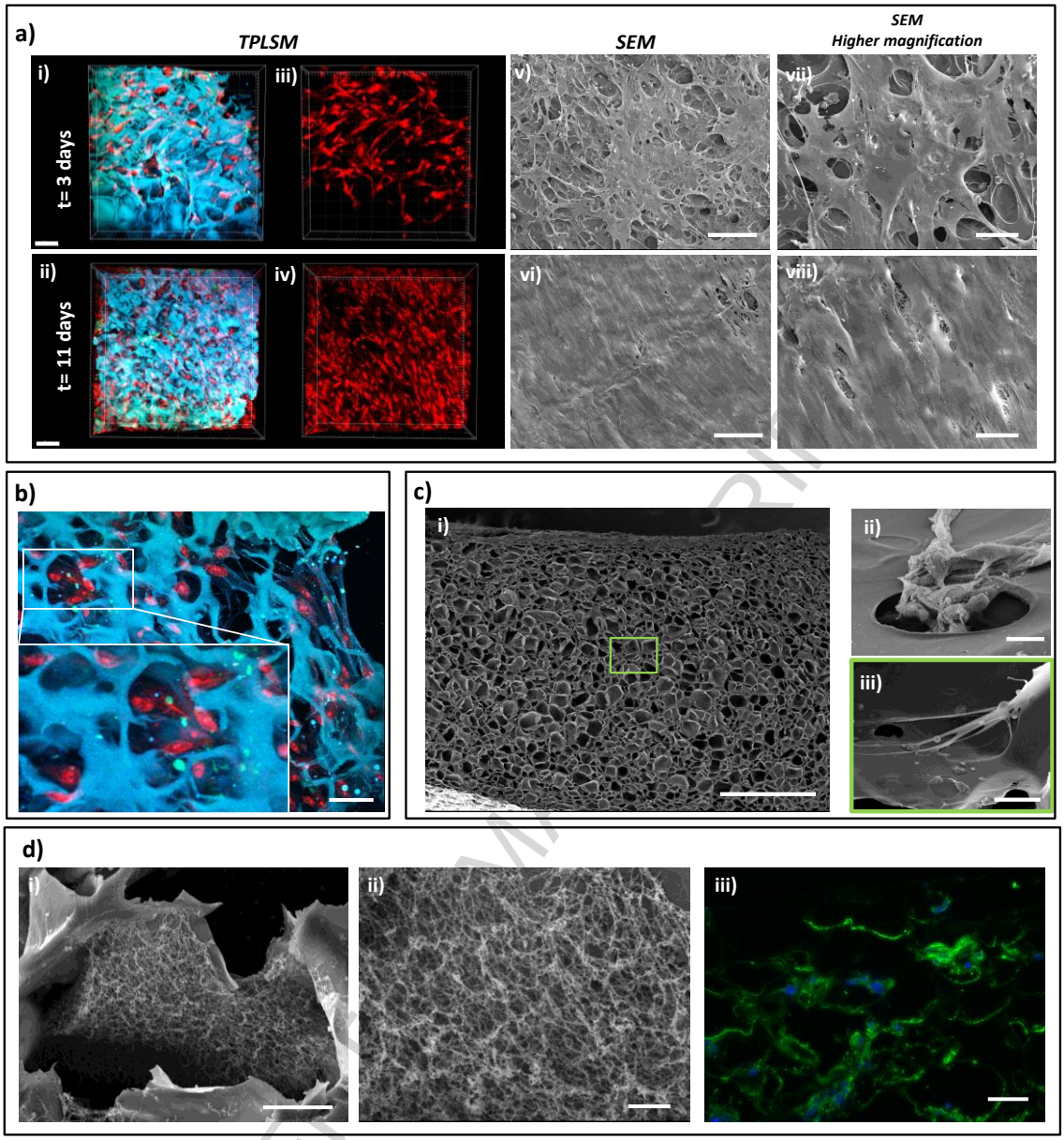

Figure 6. (a) Representative TPLSM (i to iv) and SEM (v to viii) images of HUVSMC seeded on the click-ELR scaffold prepared by the SL/GF protocol after 3 (i, iii, v, vii) and 11 days (ii, iv, vi and viii) in culture. Images (i) and (ii) corresponds with the merge of all channels, while in images (iii) and (iv) only the red channel is shown to facilitate the visualization the cells. Cells were stained with propidium iodide. The ELR-scaffold was visualized by taking advantage of its autofluorescence. (b) Detailed view of the interaction of the SMC with the macroporous click-ELR scaffold. The cells show a spread morphology, indicative of the tight interaction with the scaffold. (c) SEM image showing the porous structure of the cross-section of the click-ELR scaffold (i), the detailed view of a SMC infiltrating into a pore located on the surface of the scaffold (ii) and a zoomed in image of a representative SMC located in the inner part of the cross-section on the scaffold (iii). (d) ECM production; (i)

representative pore covered with deposited ECM; (ii) Zoomed in view of the fibrillar ECM; (iii) Immunohistochemical staining against collagen I of the cross-section of click-ELR scaffold. Scale bars (a, i-iv) 70 µm; (a, v-vi) 200 µm; (a, vii-viii) 50 µm. (b) 50 µm. (c, i) 500 µm; (c, ii) 20 µm; (c, iii) 10 µm. (d, i), 10 µm; (d, ii) 2 µm; (d, iii) 50 µm.

4. CONCLUSION

We were able to fabricate click-ELR scaffolds with interconnected porosity and supportive of cell infiltration by SL/GF technique. The macroporous structure together with the elastic nature of the ELR and the advantages of catalyst-free click chemistry make these scaffolds promising candidates for applications in tissue regeneration. Because of the fluidic nature of both gel-forming components and the ease of handling, complex 3D constructs can potentially be obtained by the injection molding technique used in this study. The recombinant nature of the ELRs allows the incorporation of further biofunctionalities in an accurate and controlled way in order to use these materials for specific applications in the biomedical field. To the best of our knowledge, this is the first time the SL/GF technique is performed in click-cross-linked systems and although demonstrated for the ELRs in this study, the protocol we developed is applicable to a large number of click systems. This gives the possibility to fully exploit such materials for tissue engineering applications where the porosity plays a crucial role in the interaction with cells and ultimately on the success of the biomaterial.

ACKNOWLEDGMENTS

This work was funded by the Excellence Initiative of the German federal and state governments in the framework of the i³tm Rotational Position Program (2014-R4-01) and by

the START-Program of the Medical Faculty of RWTH Aachen University – Fond #691713. Furthermore, the authors acknowledge the support by the core facility 2-photon Imaging, a core facility of the Interdisciplinary Center for Clinical Research (IZKF) Aachen within the Faculty of Medicine at RWTH Aachen University. J.C.R.-C. acknowledges the financial support from the following projects: MAT2013-42473-R, MAT2015-68901-R, MAT2016-78903-R, VA313U14, VA015U16 and PCIN-2015-010.

REFERENCES

[1] Loh Q L, Choong C. 2013. Three-dimensional scaffolds for tissue engineering applications: role of porosity and pore size. *Tissue Eng Part B Rev* **19** 485-502.

[2] Lutolf M P, Hubbell J A. 2005. Synthetic biomaterials as instructive extracellular microenvironments for morphogenesis in tissue engineering. *Nat Biotechnol* **23** 47-55.

[3] Yeo G C, Aghaei-Ghareh-Bolagh B, Brackenreg E P, Hiob M A, Lee P, Weiss A S. 2015. Fabricated Elastin. *Advanced healthcare materials* **4** 2530-56.

[4] Girotti A, Fernández-Colino A, López I M, Rodríguez-Cabello J C, Arias F J. 2011. Elastin-like recombinamers: Biosynthetic strategies and biotechnological applications. *Biotechnol J* **6** 1174-86.

[5] Arias F J, Santos M, Fernández-Colino A, Pinedo G, Girotti A. 2014. Recent Contributions of Elastin-Like Recombinamers to Biomedicine and Nanotechnology. *Curr Top Med Chem* **14** 819-36 (18).

[6] Sallach R E, Cui W, Balderrama F, Martinez A W, Wen J, Haller C A, Taylor J V, Wright E R, Long R C, Jr., Chaikof E L. 2010. Long-term biostability of self-assembling protein polymers in the absence of covalent crosslinking. *Biomaterials* **31** 779-91.

[7] Fernandez-Colino A, Arias F J, Alonso M, Rodriguez-Cabello J C. 2015. Amphiphilic Elastin-Like Block Co-Recombinamers Containing Leucine Zippers: Cooperative Interplay between Both Domains Results in Injectable and Stable Hydrogels. *Biomacromolecules* **16** 3389-98.

[8] de Torre I G, Wolf F, Santos M, Rongen L, Alonso M, Jockenhoevel S, Rodriguez-Cabello J C, Mela P. 2015. Elastin-like recombinamer-covered stents: Towards a fully biocompatible and non-thrombogenic device for cardiovascular diseases. *Acta Biomater* **12** 146-55.

[9] Woodhouse K A, Klement P, Chen V, Gorbet M B, Keeley F W, Stahl R, Fromstein J D, Bellingham C M. 2004. Investigation of recombinant human elastin polypeptides as non-thrombogenic coatings. *Biomaterials* **25** 4543-53.

[10] Waterhouse A, Wise S G, Ng M K, Weiss A S. 2011. Elastin as a nonthrombogenic biomaterial. *Tissue Eng Part B Rev* **17** 93-9.

[11] Urry D W. 1993. Molecular Machines: How Motion and Other Functions of Living Organisms Can Result from Reversible Chemical Changes. *Angew Chem Int Ed Engl* **32** 819-41.

[12] Rodriguez-Cabello J C, Arias F J, Rodrigo M A, Girotti A. 2016. Elastin-like polypeptides in drug delivery. *Adv Drug Delivery Rev* **97** 85-100.

[13] Nettles D L, Chilkoti A, Setton L A. 2010. Applications of elastin-like polypeptides in tissue engineering. *Adv Drug Delivery Rev* **62** 1479-85.

[14] MacEwan S R, Chilkoti A. 2014. Applications of elastin-like polypeptides in drug delivery. *Journal of controlled release : official journal of the Controlled Release Society* **190** 314-30.
[15] Gonzalez de Torre I, Santos M, Quintanilla L, Testera A, Alonso M, Rodriguez Cabello J C. 2014. Elastin-like recombinamer catalyst-free click gels: characterization of poroelastic and intrinsic viscoelastic properties. *Acta Biomater* **10** 2495-505.
[16] Nwe K, Brechbiel M W. 2009. Growing applications of "click chemistry" for bioconjugation in contemporary biomedical research. *Cancer BiotherRadiopharm* **24** 289-302.
[17] Nandivada H, Jiang X, Lahann J. 2007. Click Chemistry: Versatility and Control in the Hands of Materials Scientists. *Adv Mater* **19** 2197-208.
[18] Xi W, Scott T F, Kloxin C J, Bowman C N. 2014. Click Chemistry in Materials Science. *Adv Funct Mater* **24** 2572-90.
[19] Kolb H C, Finn M G, Sharpless K B. 2001. Click Chemistry: Diverse Chemical Function from a Few Good Reactions. *Angew Chem Int Ed Engl* **40** 2004-21.
[20] McKay C S, Finn M G. 2014. Click chemistry in complex mixtures: bioorthogonal bioconjugation. *Chem Biol* **21** 1075-101.
[21] Jiang Y, Chen J, Deng C, Suuronen E J, Zhong Z. 2014. Click hydrogels, microgels and nanogels: emerging platforms for drug delivery and tissue engineering. *Biomaterials* **35** 4969-85.
[22] Tschoeke B*, et al.* 2009. Tissue-engineered small-caliber vascular graft based on a novel biodegradable composite fibrin-polylactide scaffold. *Tissue Eng Part A* **15** 1909-18.
[23] Moreira R, Neusser C, Kruse M, Mulderrig S, Wolf F, Spillner J, Schmitz-Rode T, Jockenhoevel S, Mela P. 2016. Tissue-Engineered Fibrin-Based Heart Valve with Bio-Inspired Textile Reinforcement. *Adv Healthcare Mater* **5** 2113-21.
[24] Lee K W, Stolz D B, Wang Y. 2011. Substantial expression of mature elastin in arterial constructs. *Proc Natl Acad Sci U S A* **108** 2705-10.
[25] Murphy C M, O'Brien F J. 2010. Understanding the effect of mean pore size on cell activity in collagen-glycosaminoglycan scaffolds. *Cell Adhes Migr* **4** 377-81.
[26] Fioretta E S, Fledderus J O, Burakowska-Meise E A, Baaijens F P, Verhaar M C, Bouten C V. 2012. Polymer-based scaffold designs for in situ vascular tissue engineering: controlling recruitment and differentiation behavior of endothelial colony forming cells. *Macromol Biosci* **12** 577-90.
[27] Talacua H*, et al.* 2015. In Situ Tissue Engineering of Functional Small-Diameter Blood Vessels by Host Circulating Cells Only. *Tissue Eng Part A* **21** 2583-94.
[28] Wu W, Allen R A, Wang Y. 2012. Fast-degrading elastomer enables rapid remodeling of a cell-free synthetic graft into a neoartery. *Nat Med* **18** 1148-53.
[29] Warren P B, Huebner P, Spang J T, Shirwaiker R A, Fisher M B. 2016. Engineering 3D-Bioplotted scaffolds to induce aligned extracellular matrix deposition for musculoskeletal soft tissue replacement. *Connective tissue research* 1-13.
[30] Martin L, Alonso M, Girotti A, Javier Arias F, Carlos Rodriguez-Cabello J. 2009. Synthesis and Characterization of Macroporous Thermosensitive Hydrogels from Recombinant Elastin-Like Polymers. *Biomacromolecules* **10** 3015-22.
[31] Annabi N, Nichol J W, Zhong X, Ji C, Koshy S, Khademhosseini A, Dehghani F. 2010. Controlling the porosity and microarchitecture of hydrogels for tissue engineering. *Tissue Eng Part B* **16** 371-83.
[32] Reguera J, Urry D W, Parker T M, McPherson D T, Rodriguez-Cabello J C. 2007. Effect of NaCl on the Exothermic and Endothermic Components of the Inverse Temperature Transition of a Model Elastin-like Polymer. *Biomacromolecules* **8** 354-8.
[33] Cho Y, Zhang Y, Christensen T, Sagle L B, Chilkoti A, Cremer P S. 2008. Effects of Hofmeister anions on the phase transition temperature of elastin-like polypeptides. *J Phys Chem B* **112** 13765-71.
[34] Moreira R, Velz T, Alves N, Gesche V N, Malischewski A, Schmitz-Rode T, Frese J, Jockenhoevel S, Mela P. 2015. Tissue-engineered heart valve with a tubular leaflet design for minimally invasive transcatheter implantation. *Tissue Eng Part C* **21** 530-40.

[35] Pinho S P, Macedo E A. 2005. Solubility of NaCl, NaBr, and KCl in Water, Methanol, Ethanol, and Their Mixed Solvents. *J Chem Eng Data* **50** 29-32.
[36] Rostovtsev V V, Green L G, Fokin V V, Sharpless K B. 2002. A stepwise huisgen cycloaddition process: copper(I)-catalyzed regioselective "ligation" of azides and terminal alkynes. *Angew Chem Int Ed Engl* **41** 2596-9.
[37] Avti P K, Maysinger D, Kakkar A. 2013. Alkyne-azide "click" chemistry in designing nanocarriers for applications in biology. *Molecules* **18** 9531-49.
[38] Kennedy K M, Bhaw-Luximon A, Jhurry D. 2017. Cell-matrix mechanical interaction in electrospun polymeric scaffolds for tissue engineering: Implications for scaffold design and performance. *Acta Biomater* **50** 41-55.
[39] Lowery J L, Datta N, Rutledge G C. 2010. Effect of fiber diameter, pore size and seeding method on growth of human dermal fibroblasts in electrospun poly(epsilon-caprolactone) fibrous mats. *Biomaterials* **31** 491-504.
[40] Levental I, Georges P C, Janmey P A. 2007. Soft biological materials and their impact on cell function. *Soft Matter* **3** 299-306.
[41] Humphrey J D, Dufresne E R, Schwartz M A. 2014. Mechanotransduction and extracellular matrix homeostasis. *Nat Rev Mol Cell Biol* **15** 802-12.
[42] Discher D E, Janmey P, Wang Y L. 2005. Tissue cells feel and respond to the stiffness of their substrate. *Science* **310** 1139-43.
[43] Garcia-Arevalo C, Pierna M, Girotti A, Arias F J, Rodriguez-Cabello J C. 2012. A comparative study of cell behavior on different energetic and bioactive polymeric surfaces made from elastin-like recombinamers. *Soft Matter* **8** 3239-49.
[44] Dubuis C*, et al.* 2013. Atorvastatin-loaded hydrogel affects the smooth muscle cells of human veins. *The Journal of pharmacology and experimental therapeutics* **347** 574-81.
[45] Wilhelmi M, Jockenhoevel S, Mela P. 2014. Bioartificial fabrication of regenerating blood vessel substitutes: requirements and current strategies. *Biomed Tech (Berl)* **59** 185-95.

Graphical abstract

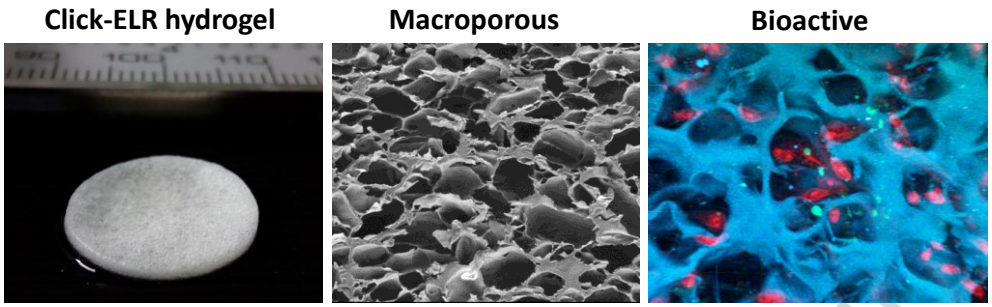

Highlights

- Strategy to apply salt-leaching/ gas foaming to click-elastin-like hydrogels.
- The resulting hydrogels featured controlled and interconnected porosity.
- Their mechanical properties compared well with those of many biological tissues.
- The hydrogels were supportive of cell-ingrowth and extracellular matrix synthesis.
- Applicable to click chemistry systems in general.